AD_____

Award Number: DAMD17-02-1-0396

TITLE: Differential Control of ErbB2 Surface Expression in Breast Cancer Cells by an Alternatively Spliced Form of ERBIN

PRINCIPAL INVESTIGATOR: Kathryn Ching

CONTRACTING ORGANIZATION: Georgetown University
Washington, DC 20007

REPORT DATE: May 2004

TYPE OF REPORT: Annual Summary

PREPARED FOR: U.S. Army Medical Research and Materiel Command
Fort Detrick, Maryland 21702-5012

REPORT DOCUMENTATION PAGE

Form Approved
OMB No. 074-0188

1. AGENCY USE ONLY (Leave blank)	2. REPORT DATE	3. REPORT TYPE AND DATES COVERED
	May 2004	Annual Summary (1 May 2003 - 30 Apr 2004)

4. TITLE AND SUBTITLE
Differential Control of ErbB2 Surface Expression in Breast Cancer Cells by an Alternatively Spliced Form of ERBIN

5. FUNDING NUMBERS
DAMD17-02-1-0396

6. AUTHOR(S)
Kathryn Ching

7. PERFORMING ORGANIZATION NAME(S) AND ADDRESS(ES)
Georgetown University
Washington, DC 20007

E-Mail: khc6@Georgetown.edu

8. PERFORMING ORGANIZATION REPORT NUMBER

9. SPONSORING / MONITORING AGENCY NAME(S) AND ADDRESS(ES)
U.S. Army Medical Research and Materiel Command
Fort Detrick, Maryland 21702-5012

10. SPONSORING / MONITORING AGENCY REPORT NUMBER

11. SUPPLEMENTARY NOTES

12a. DISTRIBUTION / AVAILABILITY STATEMENT
Approved for Public Release; Distribution Unlimited

12b. DISTRIBUTION CODE

13. ABSTRACT (Maximum 200 Words)

The ErbB2 receptor is upregulated in approximately 30% of early stage breast cancers. Persistent signaling by the receptor induces a mitogenic response in which cells continuously grow and proliferate regardless of environmental conditions. Following ligand binding and receptor activation, many cell surface receptors enter the Multivesicular Body pathway, where they are sorted and either targeted for degradation or recycled back to the plasma membrane. The specific protein-protein interactions of this pathway, and the mechanism by which sorting occurs, however, are not yet fully understood. Elucidation of the natural mechanism of ErbB2 downregulation could provide insight into the treatments and therapies given to many breast cancer patients. Here, we show that hVps20 and hSnf7, two previously undescribed proteins, are components of the MVB network and are affect cargo within the network. In addition, we also show that AIP1, a previously identified protein for its role in HIV budding, is an active participant to sorting of MVB cargo. Specifically, we show that the N-terminus of AIP1 interacts with hSnf7. Further, we show that hSnf7 can disrupt cholesterol trafficking. We continue to contribute to work done by other groups to identify and characterize the mechanism of protein trafficking.

14. SUBJECT TERMS
Vps, multivesicular body, Snf7, late endosome

15. NUMBER OF PAGES
16

16. PRICE CODE

17. SECURITY CLASSIFICATION OF REPORT	18. SECURITY CLASSIFICATION OF THIS PAGE	19. SECURITY CLASSIFICATION OF ABSTRACT	20. LIMITATION OF ABSTRACT
Unclassified	Unclassified	Unclassified	Unlimited

Table of Contents

Introduction

This study originally proposed to study the relationship between Erbin and Erb2/Her2, a member of the Epidermal Growth Factor (EGF) family of receptor tyrosine kinases. The Erbin story became less relevant, however, as studies showed that the Erbin-ErbB2 interaction is non-physiological and that Erbin likely regulates p120-catenin, as it binds this protein with ~1000 fold higher binding activity than it binds ErbB2 (Izawa, Nishizawa et al. 2002). In light of this information, we revised our aims and shifted our focus to study the mechanism of ErbB2 downregulation through targeting to the MVB pathway following receptor activation.

The EGF family of receptors integrates extracellular mitogenic signaling with intracellular signaling pathways that lead to cell proliferation and growth. These signaling cascades are closely regulated through a balance between receptor activation and receptor downregulation, which includes trafficking through the multivesicular body pathway (MVB). Targeting to the MVB pathway begins with ubquitination of the cytoplasmic tail of a given receptor following ligand binding and receptor activation. Ubiquitin is recognized by proteins of the MVB and endocytosed. The receptor then enters the vesicular network of the MVB pathway, where it is sorted amongst other endosomal cargo and then either targeted for degradation in the lysosome or proteosome, or it is recycled back to the plasma membrane (Katzmann, Odorizzi et al. 2002).

In the initiation and progression of breast cancer, the overexpression of many of these cell surface receptors disrupts the balance between activation and degradation, ultimately leading to unregulated cell proliferation and growth. ErbB2 is amplified in 30% of early-stage breast cancers and is associated with a poor prognosis (Slamon, Clark et al. 1987). When overexpressed, the receptor, like many in the EGF family, triggers increased cell proliferation through stimulation of the *ras*-MAPK pathway (Marshall 1995). Identifying the mechanisms involved in ErbB2's downregulation through MVB trafficking could provide insight into the development of new treatments and therapeutics for breast cancer patients.

As stated in Aim #1, we identified and cloned Vps32/Snf7 and Vps20 (vacuolar protein sorting), two human homologues to yeast MVB proteins, by a TBLASTN search of the EST (expressed sequence tag) database at the National Center for Biotechnology Information. We hypothesized that these human proteins, like their yeast counterparts, play critical roles in protein trafficking. In the present study, we show that Snf7 and Vps20 are found *in vivo* in complex on the surface of late endosomes. Further, we show that Snf7 is an interacting partner

of AIP1, a protein that many group have shown to be associated with the MVB pathway, but whose specific function has not yet been elucidated.

Body

Specifically, we investigated the role of two human class E Vps proteins, hVps20 and hSnf7-3. Class E proteins are critical to efficient endosomal sorting, as Vps mutants fail to transport targeted proteins to the vacuole for degradation (Raymond, Howald-Stevenson et al. 1992). More recently, studies in yeast identified three protein complexes, ESCRT-I, -II and -III (endosomal sorting complex required for transport), which are responsible for identifying, recruiting and concentrating target proteins throughout their journey in the MVB pathway (Babst, Katzmann et al. 2002). Vps20p and Snf7p are associated with the yeast ESCRT-III complex. Defects in either of these proteins results in a failure to deliver cargo to the yeast vacuole.

We identified human homologues of yeast Vps20p and Vps32p, designated hVps20 and hSnf7, by querying the NCBI EST database using yeast Vps20p and Snf7p sequences, respectively. In yeast, Vps20p and Vps32p strongly colocalize in an ESCRT-III complex. While this may suggest that the human homologues behave similarly, we found that this was not the case in overexpression studies, which followed Aim #2, as stated in the Statement of Work. Specifically, co-overexpression of hVps20 and hSnf7 blocked the formation of the large hSnf7 vesicles we observed when hSnf7 was expressed alone (see below). Rather, we observed vesicles showing an endosomal-staining pattern similar to when we expressed hVps20 alone (data not shown). Our results suggest that hVps20 and hSnf7 exist in a complex *in vivo,* but that the normal function of these proteins may be controlled, in part, by their protein levels in the cell (Peck, Bowden et al. 2003).

Using direct immunofluorescence, we observed a vesicular staining pattern with overexpressed hSnf7. Some of the vesicles observed were unusually large (data not shown). The nature of these vesicles were most likely late endosomes/ lysosomes, as co-expression of hSnf7 with an ATPase defective Vps4-A mutant, a known marker of late endosomes/ lysosomes, revealed complete co-localization of the two proteins (Fig. 1). This staining pattern is not unexpected, given previously reported yeast data. Using flipin to stain for cholesterol, we also observed enrichment of cholesterol within hSnf7 containing vesicles compared to cholesterol staining in untransfected cells (data not shown).

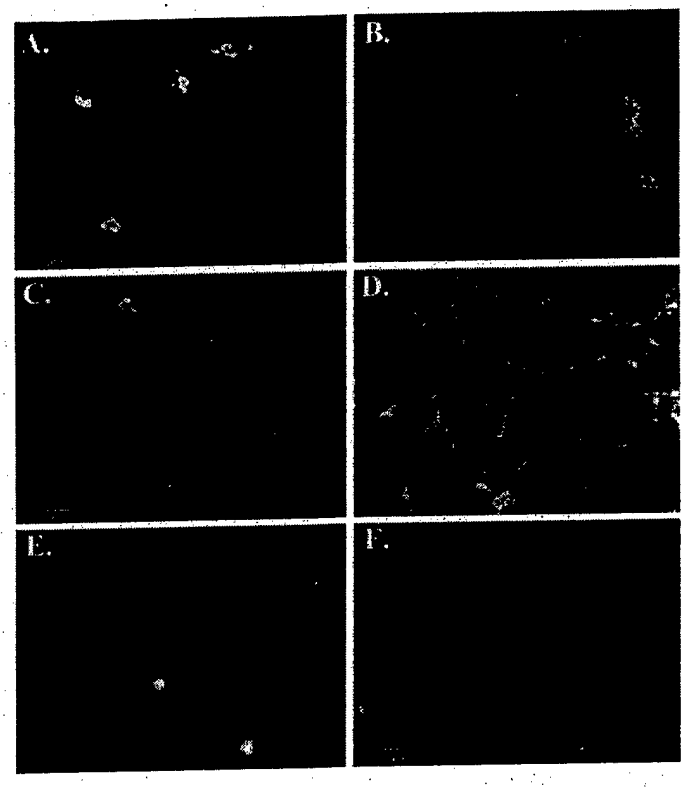

Figure 1: hSnf7 colocalizes with an ATPase defective Vps4-A mutant. HeLa cells were co-transfected with either FLAG-tagged hSnf7 alone (A and B) or myc-tagged Vps4-A ATPase mutant (C and D) or co-transfected with FLAG-tagged hSnf7 and myc-tagged Vps4-A ATPase mutant (E and F). Cells were stained with mouse anti-FLAG antibodies (A and F), monoclonal anti-myc antibodies (C and E), monoclonal anti-EEA1 antibody (B) or for F-actin with Texas Red-conjugated Phalloidin (D).

Using a glutathione S-transferase-capture strategy, we tested for other possible interacting partners of hSnf7. We identified mouse AIP1 (Apoptosis-linked gene 2 Interacting Protein 1) as a hSnf7 interacting partner, and confirmed this interaction by immunoprecipitation (Fig. 2). When we co-expressed hSnf7 and AIP1 in HeLa cells, we observed , by direct immunofluorescence, colocalization of the two proteins in a vesicular staining pattern (Fig. 3). We mapped the interaction between AIP1 and Bro1 to the N-terminal region of AIP1, which contains both a Bro1 and an α-helical domain, both of which are required for its interaction with hSnf7 (Fig. 3 and data not shown).

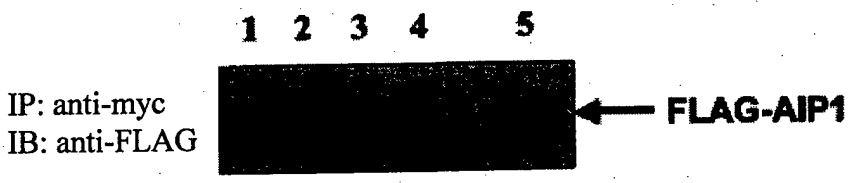

Figure 2: FLAG-tagged AIP1 and myc-tagged hSnf7 interact *in vivo* as demonstrated by co-immunoprecipitation form HeLa lysates. Cell lysates were prepared from untransfected cells (lane 1), cells transfected with pcDNA-myc vector and FLAG-tagged AIP1 (lane 2), cells transfected with myc -tagged hSnf7 and FLAG-tagged RPH-2 (lane 3), or from cells transfected with myc-tagged hSnf7 and FLAG-tagged AIP1 (lane 4). AIP1 input is shown in lane 5.

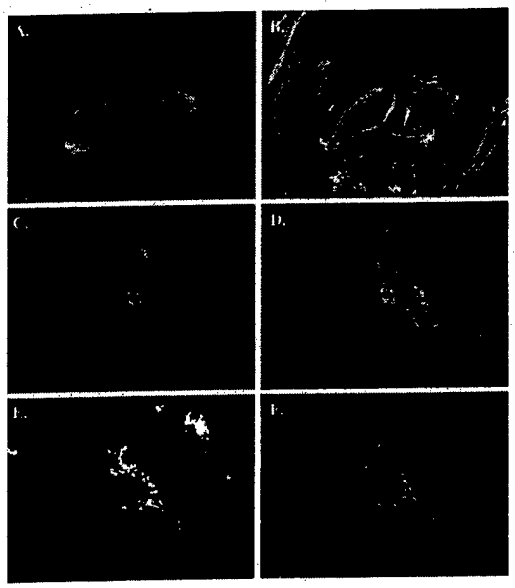

Figure 3: AIP1 colocalizes with hSnf7 in vesicular structures. HeLa were transfected with myc-tagged hSnf7 (A), cotransfected with myc-tagged hSnf7 (C) and FLAG-tagged AIP1 (D), or with myc-Snf7 (E) and FLAG-tagged AIP-N- Δ1. Actin was visualized by staining with Texas Red-conjugated pahllodin (B).

AIP1 was identified as a part of the MVB machinery in studies of HIV and the Equine Infectious Anemia virus. Both viruses utilize cellular components of the MVB to bud from the plasma membrane of infected cells, and several groups demonstrated that cellular AIP1 binds a YPXL tetra-residue motif found on the gag proteins of both viruses during this budding process (Strack, Calistri et al. 2003). However, AIP1's natural cellular target containing this motif has yet to be identified. We identified hvam6 through a BLAST search as containing a YPDL motif. Previous studies show that hvam6 is required for fusion of late endosomes with lysosomes (Caplan, Hartnell et al. 2001). Using a GST-capture approach, our preliminary results indicate that FLAG-AIP1 binds a recombinant, truncated construct of hvam6, designated hvam6Δ , containing the YPDL motif (Fig. 4).

Figure 4: FLAG-AIP1 binds GST-vam6Δ. Cell lysates were prepared from HeLa cells transfected with FLAG-AIP1 and incubated with either GST-Cdc42 (lane 1) or GST-vam6Δ (lane 2) for specific capture. FLAG-AIP1 input is shown in lane 3.

We are currently investigating AIP1's binding affinity to a hvam6Δ mutant containing a proline to alanine substitution. We are currently trying to optimize our lysis and washing conditions for this experiment.

Key research accomplishments

*We have shown that hSnf7 localizes to late endosomes/ lysosomes.

*GST capture and coimmunoprecipitation experiments show that hSnf7 interacts with the N-terminus of AIP1.

*The interaction between AIP1 and hSnf7 requires the Bro1 and α-helical domains of AIP1.

*Direct immunofluorescence reveals that hSnf7 and AIP1 colocalize at late endosomes/ lysosomes.

*Preliminary data indicates that hvam6 is an interacting partner of AIP1.

Reportable Outcomes

- Paper published entitled "Structure and function of human Vps20 and Snf7 proteins" in the Biochemical Journal, Feb. 1 (377), 693-700.
- Second author on published review entitled "Cdc42 Regulates Diverse Signaling Pathways in Mammalian Cells."
- Seminar in the Department of Biochemistry and Molecular Biology at Georgetown University Medical Center
- Contributed to a manuscript in preparation entitled "Global Genomic Approaches to the Study of Human Gene Function."

Conclusions

We have identified and published on two human Vps proteins, hVps20 and hSnf7, that are part of the MVB machinery. Following the MVB story for the ErbB2 receptor has taken our research on a path to identify several components of the MVB machinery and to investigate the protein-protein interactions that are responsible for targeting and sorting cargo in the MVB pathway. We continue to study other cellular interacting partners of AIP1, such as its well-documented relationship with Tsg101 and our potential interacting partner, hvam6. The outcome of these various studies has the potential to give us significant insight into receptor trafficking and downregulation.

Biochem. J. (2004) 377, 693–700 (Printed in Great Britain)

Structure and function of human Vps20 and Snf7 proteins

Jeremy W. PECK[1], Emma T. BOWDEN[1] and Peter D. BURBELO[2]

Lombardi Comprehensive Cancer Center, Georgetown University Medical Center, Washington, DC 20057, U.S.A.

Snf7p (sucrose non-fermenting) and Vps20p (vacuolar protein-sorting) are small coil-coiled proteins involved in yeast MVB (multivesicular body) structure, formation and function. In the present study, we report the identification of three human homologues of yeast Snf7p, designated hSnf7-1, hSnf7-2 and hSnf7-3, and a single human Vps20p homologue, designated hVps20, that may have similar roles in humans. Immunofluorescence studies showed that hSnf7-1 and hSnf7-3 localized in large vesicular structures that also co-localized with late endosomal/lysosomal structures induced by overexpressing an ATPase-defective Vps4-A mutant. In contrast, overexpressed hVps20 showed a typical endosomal membrane-staining pattern, and co-expression of hVps20 with Snf7-1 dispersed the large Snf7-staining vesicles. Interestingly, overexpression of both hSnf7 and hVps20 proteins induced a post-endosomal defect in cholesterol sorting. To explore possible protein–protein interactions involving hSnf7 proteins, we used information from yeast genomic studies showing that yeast Snf7p can interact with proteins involved in MVB function. Using a glutathione S-transferase-capture approach with several mammalian homologues of such yeast Snf7p-interacting proteins, we found that all three hSnf7s interacted with mouse AIP1 [ALG-2 (apoptosis-linked gene 2) interacting protein 1], a mammalian Brolp [BCK1 (bypass of C kinase)-like resistance to osmotic shock]-containing protein involved in cellular vacuolization and apoptosis. Whereas mapping experiments showed that the N-terminus of AIP1 containing both a Brol and an -helical domain were required for interaction with hSnf7-1, Snf7-1 did not interact with another human Brol-containing molecule, rhophilin-2. Co-immunoprecipitation experiments confirmed the *in vivo* interaction of hSnf7-1 and AIP1. Additional immunofluorescence experiments showed that hSnf7-1 recruited cytosolic AIP1 to the Snf7-induced vacuolar-like structures. Together these results suggest that mammalian Vps20, AIP1 and Snf7 proteins, like their yeast counterparts, play roles in MVB function.

Key words: ALG-2 (apoptosis-linked gene 2) interacting protein 1 (AIP1/ALIX), charged multivesicular body protein (CHMP4), late endosome, multivesicular body, Snf7, Vps.

INTRODUCTION

The proteins and signalling pathways involved in protein trafficking in humans are relatively unknown in comparison with yeast, for which detailed models are available [1]. In humans, one of the best-understood processes involving protein trafficking is ligand-induced down-regulation of mitogenic receptors, which involves receptor endocytosis via clathrin-coated vesicles [1]. The subsequent sorting of endocytosed receptors for recycling to the cell surface or to lysosomes for degradation occurs in a complex, multi-step process that requires re-localization to the internal vesicles of late endosomes or MVB (multivesicular bodies) [2]. More than 20 yeast proteins, the class E Vps (vacuolar protein-sorting) proteins, are important for endosomal sorting, as shown by Vps mutants that fail to transport efficiently newly synthesized hydrolases to vacuoles [3]. More recently, yeast studies identified three protein complexes, termed ESCRT-I, -II and -III (endosomal sorting complex required for transport), which are involved in the sequential processing of ubiquitinylated endosomal membrane proteins for inclusion into the MVB pathway [4,5]. ESCRT-I is involved in binding the ubiquitinylated cargo and activates ESCRT-II, which then assembles the ESCRT-III complex on internal endosomal membranes before the formation of a new vesicle within the MVB cargo [4,5]. The yeast ESCRT-III complex is composed of at least four proteins, Snf7p (sucrose non-fermenting, also known as Vps32), Vps2p, Vps20p and Vps24p [5]. Mutations in each of these four yeast genes show defects in the late endosome to MVB transition and thus do not deliver target proteins to the yeast vacuole. The Vps20p–Snf7p subcomplex is associated with the late endosome membrane and Vps2p plus Vps24p appears to bind the membrane-bound Vps20p–Snf7p complex.

Snf7p is a relatively small, charged, coiled-coil protein, which was originally identified genetically in a screen for mutants unable to sense glucose concentration changes [6,7]. Consistent with a role for Snf7p in MVB formation and other signalling pathways that may or may not require protein trafficking, large-scale yeast genomic and proteonomic studies suggest that Snf7p may interact with multiple proteins including Vps4p [8–10], Rim13p [9] and Rim20p [9]. One of these components, Rim20p, is a scaffold protein required for proteolytic activation of a transcription factor needed for mediating pH transcriptional responses in *Saccharomyces cerevisiae* [11]. Interestingly, this interaction between yeast Snf7p and Rim20p is functionally and evolutionarily conserved with fungal homologues from *Aspergillus nidulans* [12], where the Rim20p homologue (PalA) functions to assemble a complex required for proteolytic cleavage of a transcription factor involved in alkaline pH adaptation [12,13]. Whereas in yeast, a second related Rim20p/PalA molecule, Brolp [BCK1 (bypass of C kinase)-like resistance to osmotic shock], is known, additional homologues for these molecules have been identified in amphibians [14], mice [15,16] and humans

Abbreviations used: AIP1, ALG-2 interacting protein 1; Brol, BCK1 (bypass of C kinase)-like resistance to osmotic shock; CHMP4, charged multivesicular body protein; EEA1, early endosome antigen 1; ESCRT, endosomal sorting complex required for transport; EST, expressed sequence tag; GST, glutathione S-transferase; LAMP, lysosome-associated membrane protein; MVB, multivesicular body; RPH-2, rhophilin-2; Snf, sucrose non-fermenting; Vps, vacuolar protein-sorting.

[1] These authors contributed equally to this work.

[2] To whom correspondence should be addressed (e-mail burbelpd@georgetown.edu).

[12,17]. The function of these homologues is still not completely understood, but the mouse homologue, AIP1 [ALG-2 (apoptosis-linked gene 2) interacting protein 1, also known as ALIX and probably a homologue of yeast Bro1p], was originally identified in a yeast two-hybrid screen as being capable of interacting with a protein, ALG-2, involved in apoptosis [15,16]. Overexpression of the AIP1 C-terminus has at least two seemingly different biological effects, including inhibiting cell death [15,18] and inducing vacuolization [19], possibly via interactions with SH3 (Src homology 3 domain)-containing molecules SETA (SH3-containing protein expressed in tumorigenic astrocytes)/RUK (regulator of ubiquitous kinase) [18,20] and endophilins [19] respectively. Although AIP1 and these other Rim20p/PalA homologues have Bro1 domains, the function of the Bro1 domain is not known.

In the present study, we have characterized one and three human homologues respectively of the yeast late endosomal ESCRT-III complex proteins, Vps20p and Snf7p. Human hVps20 is 44 % similar to its yeast counterpart, and hSnf7-1, hSnf7-2 and hSnf7-3 are approx. 50 % similar to yeast Snf7p. Immunofluorescence studies showed that overexpressed recombinant hSnf7 proteins co-localized with lysosomes, whereas hVps20 showed a more endosomal membrane-staining pattern. Co-expression studies showed that hVps20 expression dispersed hSnf7 vesicles. Interestingly, cells expressing either hSnf7 or hVps20 proteins induced a post-endosomal defect in cholesterol sorting. Using affinity-capture experiments and co-immunoprecipitation, we show that hSnf7 proteins interact with mouse AIP1, a protein known to be involved in cellular vacuolization. Whereas the Bro1 domain of AIP1 was required for its interaction with hSnf7 proteins, hSnf7 proteins did not interact with RPH-2 (rhophilin-2), another human Bro1-containing protein. Furthermore, co-immunofluorescence studies revealed that AIP1 was recruited to hSnf7-1-containing vesicles. These results suggest that hVps20, hSnf7 and mammalian homologues of AIP1, similar to their yeast counterparts, may play important roles in MVB formation and function.

MATERIALS AND METHODS

Identification and cloning of human Vps20 and Snf7 proteins

Human Snf7 clones were identified from a TBLASTN search of the EST (expressed sequence tag) database at the National Center for Biotechnology Information (http://www.ncbi.nlm.nih.gov) using the protein sequence of yeast Snf7p as a query. One of these human EST clones, designated human hSnf7-1, was obtained from the IMAGE consortium (Livermore, CA, U.S.A.; Clone ID no. 4751943). This clone was sequenced on an Applied Biosystem 377 DNA sequencer and has GenBank® accession no. AY329084. Clones containing related genes, designated human Snf7-2 and Snf7-3, were obtained from the IMAGE consortium (Clone ID nos. 5173394 and 4356570 respectively). A similar approach using yeast Vps20p was used to identify and obtain a human Vps20 clone (Clone ID no. 4751943). The GenBank® accession nos. of hSnf7-2, hSnf7-3 and hVps20 are AY329085, AY329086 and AY329087 respectively.

Mammalian expression vectors for hSnf7 proteins, hVps20, Vps4a, PalBH, RPH-2 and AIP1

The coding sequence of hSnf7-1 was amplified by PCR from the corresponding cDNA clone using the two primers 5′-GAGGGATCCAGTGGTCTCGGCAGGCT-3′ and 5′-GAGCTCGAGTCAGGATACCCACTCAGC-3′ and then subcloned in-frame into the *Bam*HI–*Xho*I sites downstream of a cytomegalovirus-driven N-terminal Myc epitope-tagged pcDNA3 mammalian expression vector. The hSnf7-3 coding sequence was amplified by PCR using the *Bam*HI–*Xho*I linker primer pairs 5′-GAGGGATCCAGCAAGTTGGGCAAGTTC-3′ and 5′-GAGCTCGAGTTAGGTAGCCCAAGCTGC-3′ and subcloned in-frame into the *Bam*HI–*Xho*I sites of the cytomegalovirus-driven N-terminal FLAG-tagged pCAF2 mammalian expression vector [21]. The coding sequence of hVps20 was amplified using two *Bgl*II–*Xho*I linker primers 5′-GAGAGATCTGCCATGGGTAACCTGTTC-3′ and 5′-GAGCTCGAGTGAAGCCGCCACCAGCTC-3′, and the corresponding cDNA was used to generate a C-terminal Myc-tagged construct. A pcDNA-Myc-tagged Vps4-A mammalian expression vector was a gift from Dr M. Negishi (Kyoto University, Tokyo, Japan). An N-terminal Myc-tagged mammalian expression vector for PalBH [22] was a gift from Dr T. Maeda (University of Tokyo, Tokyo, Japan). A pCAF1–RPH-2 mammalian expression vector was also used as described in [21]. Full-length mouse FLAG epitope-tagged AIP1 mammalian expression vector [15] was a gift from Dr L. D'Adamio (Albert Einstein College of Medicine, Bronx, NY, U.S.A.). Additional AIP1 fragments were generated by PCR and subcloned to generate the following AIP1 mutants in the FLAG-tagged pCAF vector by PCR amplification: AIP1-N-Δ1 (amino acids 1–445), AIP1-N-Δ2 (amino acids 1–208), AIP1-N-Δ3 (amino acids 182–445) and AIP1-C-Δ1 (amino acids 436–869).

Immunofluorescence

Immunofluorescence of HeLa cells was performed essentially as described in [21]. HeLa cells were fixed and permeabilized, 24 h after transfecting with FuGENE 6 transfection reagent (Roche Molecular Biochemicals, Indianapolis, IN, U.S.A.). Coverslips were stained with the appropriate anti-epitope antibodies, including mouse anti-FLAG™ M2 (Sigma, St. Louis, MO, U.S.A.), polyclonal anti-FLAG™ antibody (Sigma) and mouse anti-Myc monoclonal antibody (Sigma). Mouse monoclonal antibodies to EEA1 (early endosome antigen 1) and LAMP-1 (lysosome-associated membrane protein-1) were obtained from Transduction Laboratories (Lexington, KY, U.S.A.). Lysotracker™ was obtained from Molecular Probes (Eugene, OR, U.S.A.). Fluorescein-conjugated goat anti-mouse IgG (Rockland Immunochem, Gilbertsville, PA, U.S.A.), Texas-Red-conjugated anti-mouse (Jackson Immunoresearch Laboratories, West Grove, PA, U.S.A.) and FITC-conjugated goat-anti-rabbit (Rockland Immunochem) antibodies were used as secondary antibodies. Texas Red-conjugated Phalloidin (Sigma) was used to stain F-actin.

For cholesterol staining, cells were incubated in PBS containing 10 μg/ml of flipin complex (Sigma). Confocal microscopy was performed with an Olympus Fluoview confocal microscope (Olympus America, Melville, NY, U.S.A.) attached to an Olympus 1 × 70 inverted fluorescent scope equipped with a 60× oil immersion lens. Digitalized images were captured using the Fluoview software (Olympus America). The pictures of cells showing cholesterol were taken on a Nikon E600 epifluorescent microscope.

Production of recombinant proteins

GST (glutathione S-transferase) fusion constructs for several of the proteins, including full-length hSnf7-1 (GST-hSnf7-1; amino acids 2–222), hSnf7-3 (GST-hSnf7-3; amino acids 2–234) and hVps20 (GST-hVps20; amino acids 2–201), were created using the *Bam*HI–*Xho*I sites of pGEX4T3 and the cDNAs generated above for the mammalian expression vectors. For hSnf7-2, the amino acids 2–224 were amplified using two *Bgl*II–*Xho*I linker primers 5′-GAGAGATCTTCGGTGTTCGGGAAGCTG-3′ and

5′-GAGCTCGAGTTACATGGATCCAGCCCA-3′, and the corresponding PCR product was subcloned into the *Bam*HI–*Xho*I site of pGEX-4T3. A pGEX-Vps4-A bacterial expression vector was a gift from Dr M. Negishi. Recombinant GST fusion constructs were produced in *Escherichia coli*, purified on glutathione–agarose beads as described previously [23] and left attached to the beads.

GST-capture experiments

GST-affinity-capture experiments were used to screen for potential protein–protein interactions between hSnf7 proteins and hVps20, Vps4-A, PalBH, RPH-2 and AIP1. Briefly, 100 mm^2 dishes of Cos-1 cells were transfected with the different constructs encoding hSnf7-1, hSnf7-3, hVps20, Vps4-A (wild-type and ATPase mutant), PalBH, RPH-2 and AIP1, using FuGENE 6 transfection reagent (Roche Molecular Biochemicals). Cos1 cells were lysed 24 h post-transfection in a buffer containing 50 mM Tris (pH 7.2), 1 % (v/v) Triton X-100, 200 mM NaCl, 10 mM $MgCl_2$ and protease inhibitors. Lysates were then spun down for 15 min at 14 000 *g* to pellet insoluble material, precleared with GST bound to glutathione beads, and then the soluble fraction was incubated for 1 h at 4 °C with the respective immobilized GST-recombinant protein. In these studies, approx. 1 μg of GST or GST-fusion proteins was used. The beads were then washed, resuspended in SDS/PAGE sample buffer, run on an SDS/polyacrylamide gel, transferred to nitrocellulose and then subjected to Western blotting.

Immunoprecipitation

Cos1 cells were transfected with FuGENE 6 transfection reagent containing plasmids encoding FLAG-epitope-tagged AIP1 and Myc-tagged Snf7-1. Additional control constructs, including FLAG-epitope-tagged RPH-2 were also tested. Cell lysates were prepared 48 h after transfection from these transfected cells and from control untransfected cells. These lysates were then incubated for 1 h with the anti-Myc antibody. After the antibody incubation, Protein A/G-coupled agarose beads were added to each sample for an additional 1 h. After washing, the captured proteins were separated on a SDS/10 % polyacrylamide gel and transferred to nitrocellulose. The immobilized proteins were probed with a polyclonal anti-FLAG™ antibody (Sigma) followed by an anti-rabbit horseradish peroxidase secondary antibody conjugate. After washing, the blot was developed with ECL® (enhanced chemiluminescence) reagents (Pierce, Rockford, IL, U.S.A.) and exposed to X-ray film.

RESULTS

Identification of human homologues of yeast Snf7p and Vps20p

Using the human EST databases, we searched for human proteins homologous with the yeast Snf7p. In contrast with yeast, three human Snf7 homologues were identified (Figure 1A). Plasmids containing cDNAs for these human proteins, designated hSnf7-1, hSnf7-2 and hSnf7-3, were obtained from the IMAGE consortium, sequenced and confirmed to encode proteins of 222, 224 and 234 amino acid residues respectively (Figure 1A). Comparisons of the amino acid sequences of hSnf7-1, hSnf7-2 and hSnf7-3 with yeast Snf7p revealed that they were 49, 50 and 49 % similar over 206, 217 and 230 residues respectively (Figure 1A). Secondary-structure analysis programmes revealed that all three human Snf7 homologues, similar to yeast Snf7p, have amino acid sequences that probably fold into coiled-coil secondary structures (results not shown). At the time of submission to GenBank®,

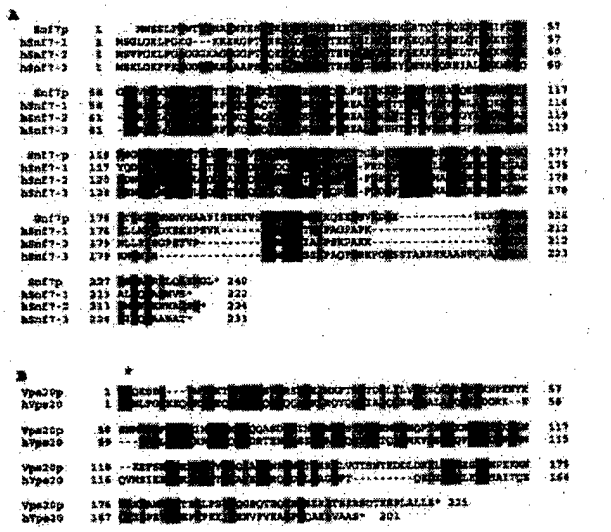

Figure 1 Identification of human homologues of yeast Snf7p and Vps20p

TBLASTN searches of the human EST database identified human homologues of yeast Snf7p and Vps20p. The numbers at the beginning and end of each line indicate the total number of amino acid residues to that point in the sequence. Optimal alignment of different proteins was performed using the AlignX function of the VectorNTI Suite (version 6.0.5) software (InforMax). (**A**) Three different human homologues (hSnf7-1, hSnf7-2, and hSnf7-3) of yeast Snf7p were identified. Amino acids within human Snf7 proteins that were identical or conserved amino acids with Snf7p from *S. cerevisiae* are shown in dark and light shading respectively. (**B**) A single human Vps20 homologue (hVps20) of Vps20p from *S. cerevisiae* was identified. Human amino acids identical or conserved with Vps20p from *S. cerevisiae* are shown in dark and light shading respectively. *, Glycine residue myristoylated in yeast Vps20p and the corresponding residue probably modified in hVps20.

only one human yeast Snf7p homologue, designated as CHMP4a (charged MVB protein), was known but not characterized [24], although a contemporaneous study by Katoh et al. [25] identified CHMP4A and CHMP4B proteins as corresponding to hSnf7-2 and hSnf7-1 respectively.

Vps20p is a yeast protein [6], which forms a complex with Snf7p [5]. We identified only a single Vps20p homologue in the human EST database. The 201-amino-acid protein encoded by this human cDNA, designated hVps20, is similar in size and sequence (44 % similarity) to yeast Vps20p (Figure 1B). Human Vps20, similar to yeast Vps20p, which is known to be myristoylated [5], contains a typical N-terminal consensus sequence (MGDLFGRKK) for myristoylation and also probably forms coiled-coil secondary structures (results not shown). Finally, additional structural analysis showed that the human homologues of Vps20 and Snf7 are less similar to each other than the yeast prototypes (results not shown).

Overexpressed hSnf7 proteins localize to late endosomes/lysosomes

We expressed epitope-tagged hSnf7-1 and hSnf7-3 in HeLa cells and examined their localization by immunofluorescence. Both N-terminal epitope-tagged hSnf7-1 (Figures 2A and 2B) and hSnf7-3 (Figures 2C and 2D) localized to vesicular-like structures in HeLa cells, some of which were unusually large. Cells co-expressing hSnf7-1 and hSnf7-3 showed complete co-localization to these large vesicular structures (Figures 2E and 2F). Overexpression of these hSnf7 proteins did not appear to be toxic, as judged by abnormal morphological changes, such as cell blobbing, which would be suggestive of non-specific toxicity.

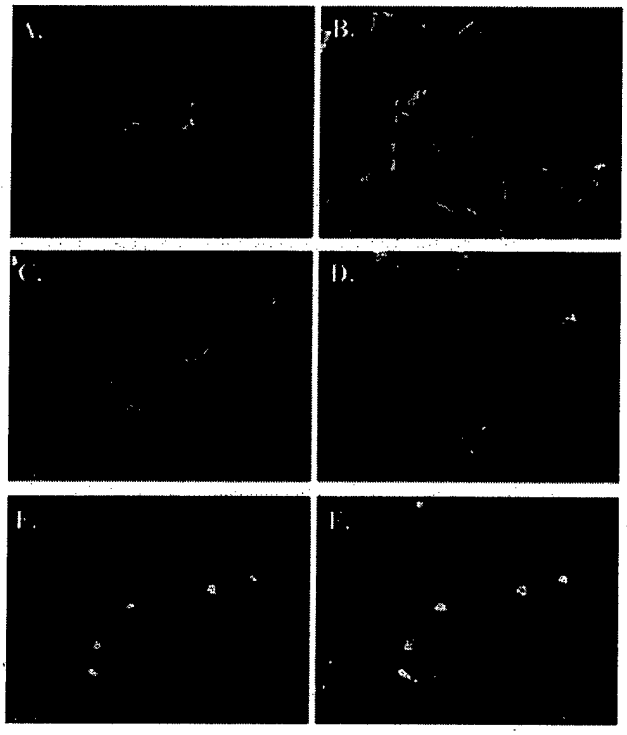

Figure 2 Expression of hSnf7-1 and hSnf7-3 in HeLa cells

Cells were transfected with either N-terminal Myc-tagged hSnf7-1 (**A**, **B**) or FLAG-tagged hSnf7-3 (**C**, **D**) or co-transfected with Myc-tagged hSnf7-1 and FLAG-tagged hSnf7-3 (**E**, **F**). The cells were fixed 24 h after transfection, permeabilized and stained. hSnf7-1 (**A**) and hSnf7-3 (**C**) were detected with mouse monoclonal anti-Myc and anti-FLAG monoclonal antibodies respectively, followed by staining with an FITC-conjugated goat anti-mouse antibody. F-actin was detected using Texas Red-conjugated phalloidin (**B**, **D**). In the co-transfected cells, a mouse anti-Myc monoclonal antibody was used to detect hSnf7-1 protein (**E**), whereas a rabbit anti-FLAG polyclonal antibody was used to stain for hSnf7-3 protein (**F**).

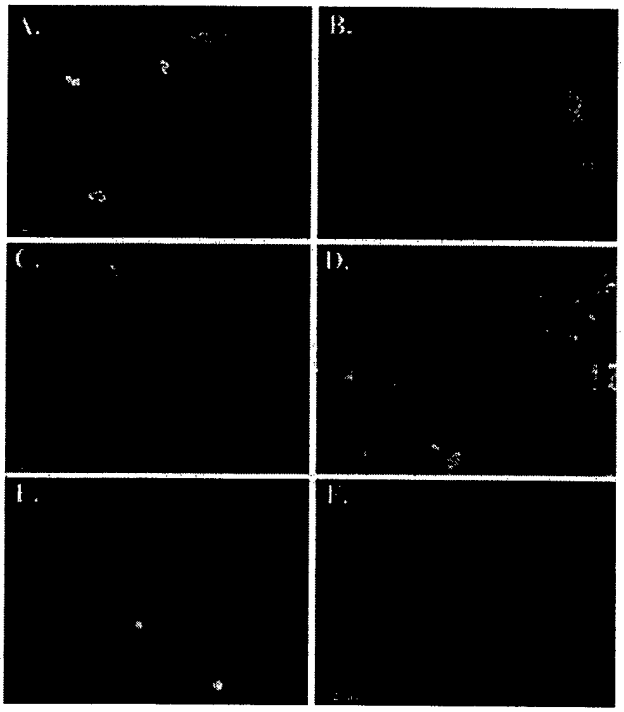

Figure 3 hSnf7 proteins co-localize with an ATPase-defective Vps4-A mutant

HeLa cells were co-transfected with either the FLAG-tagged hSnf7-3 alone (**A**, **B**) or Myc-tagged Vps4-A ATPase mutant alone (**C**, **D**), or co-transfected with FLAG-tagged hSnf7-3 and Myc-tagged Vps4-A ATPase mutant (**E**, **F**). The cells expressing FLAG-tagged hSnf7-3 (**A**, **F**) and Myc-tagged Vps4A (**C**, **E**) were fixed 16 h after transfection, permeabilized and stained with a polyclonal anti-FLAG antibody and a mouse anti-Myc monoclonal antibody. Cells were also stained with a monoclonal anti-EEA1 antibody (**B**) for F-actin with Texas Red-conjugated phalloidin (**D**).

However, interestingly, approx. 25 % of the hSnf7-3 overexpressing cells showed alterations of their F-actin-staining pattern (Figure 2D), which was not observed in the hSnf7-1 overexpressing cells (Figure 2A).

To identify the nature of these large hSnf7-containing vesicles, we used several different markers for vesicles involved in protein trafficking, including an anti-EEA1 antibody, a marker for early endosomes, and LysoTracker, a marker of late endosomes. Whereas HeLa cells expressing hSnf7-3 showed the large vesicles in the perinuclear region (Figure 3A), these vesicles, while in a similar location with EEA1-staining endosomes (Figure 3B), did not show significant co-localization. Additionally, we attempted to use anti-LAMP-1 antibodies, but the immunofluorescence staining of endogenous LAMP-1 was poor in these HeLa cells (results not shown). In the light of previous studies showing that an ATPase-defective mutant of Vps4-A induced similar abnormally large vacuolar-like structures that were late endosomes/lysosomes [26], we tested the expression of an ATPase-defective mutant rat Vps4-A(E/Q) construct and found that overexpression of this mutant protein by itself induced vesicle-like structures in HeLa cells (Figures 3C and 3D), which were morphologically similar to those produced by overexpressed hSnf7-1 and hSnf7-3. Interestingly, overexpression of the Vps4-A mutant with hSnf7-3 caused the hSnf7-3 (Figures 3E and 3F) or hSnf7-1 (results not shown) protein to localize to the Vps4-A-induced endosomal structures. Taken together, these results suggest that Snf7-containing structures probably represent late endosomes/lysosomes and that Vps4-A might normally regulate hSnf7 protein localization and/or function.

Overexpressed hVps20 shows a cellular localization pattern that is distinct from hSnf7 proteins

The localization pattern of overexpressed hVps20 was also examined in HeLa cells. To avoid potentially disrupting access to or the biological activity of the N-terminal myristoylation sequence of hVps20, the cDNA encoded by this protein was tagged at its C-terminus. Overexpression of this tagged hVps20 construct produced a diffuse membranous staining pattern in HeLa cells (Figures 4A and 4B), which showed some co-localization with early endosomes (results not shown). In light of yeast studies showing that Vps20p and Snf7p are in an ESCRT-III complex required for MVB formation [5], we examined HeLa cells overexpressing both hVps20 and hSnf7 proteins. Interestingly, co-expression of hVps20 with hSnf7-3 often blocked the accumulation of the large hSnf7-3-staining vesicles, and instead yielded more vesicles showing the endosomal-staining pattern seen with hVps20 alone that strongly co-localized with each other (Figures 4C and 4D). Specifically, approx. 40 % of the co-transfected cells showed dispersion of the large Snf7 vesicles. These results were not observed with the expression of other unrelated proteins or when different concentrations of Snf7-3 expression vector were used (results not shown). These results potentially suggest that hVps20 and hSnf7 proteins are probably part of a larger protein complex *in vivo* and that the levels of these different proteins may be important in controlling their normal function.

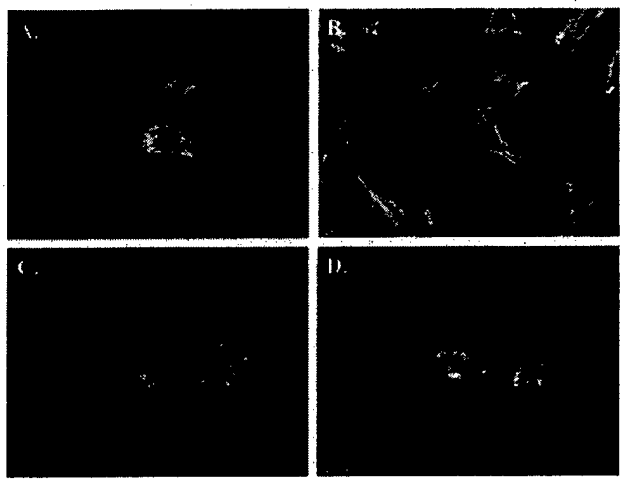

Figure 4 Localization of hVps20 to endosomes showing a dominant staining pattern when co-expressed with hSnf7-3

Cells were transfected with C-terminal Myc-tagged hVps20 (**A**, **B**) or co-transfected C-terminal Myc-tagged hVps20 and FLAG-tagged Snf7-3 (**C**, **D**). The cells were fixed 24 h after transfection, permeabilized and stained. hVps20 (**A**) was detected with mouse monoclonal anti-Myc antibody followed by staining with an FITC-conjugated goat anti-mouse antibody. F-actin was detected using Texas Red-conjugated phalloidin (**B**). Co-transfected cells were stained for Myc-tagged hVps20 (**C**) and FLAG-tagged Snf7-3 (**D**).

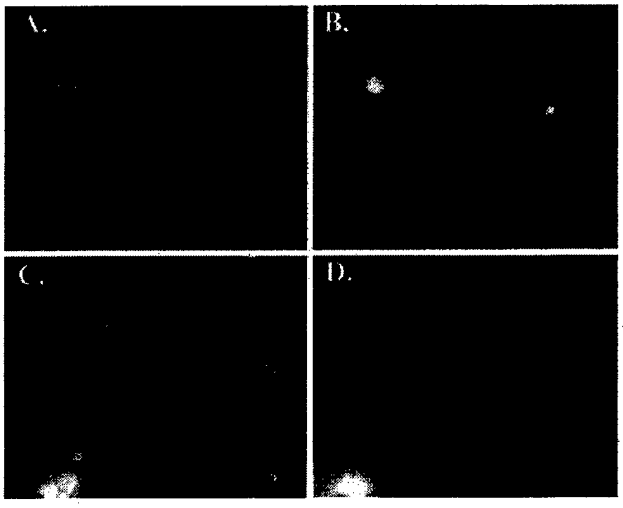

Figure 5 hSnf7 and hVps20 expression alters cholesterol trafficking

Cells were transfected with either FLAG-tagged hSnf7-3 (**A**, **B**) or C-terminal Myc-tagged hVps20 (**C**, **D**). The cells were fixed 24 h after transfection, permeabilized and stained for FLAG-tagged hSnf7-3 (**A**) or Myc-tagged hVps20 (**C**). Flipin was used to stain cholesterol (**B**, **D**).

hVps20 and hSnf7 proteins alter cholesterol trafficking

Since the overexpression of two different human Snf7 proteins induced vesicular structures, which morphologically resembled late endosomes/lysosomes induced by a Vps4-A mutant that is known to disrupt cholesterol trafficking [26], we examined whether cholesterol trafficking was altered in the Snf7-expressing cells, using flipin to stain for cholesterol. As might be predicted, cells showing accumulation of hSnf7 vesicular structures showed a marked enrichment for cholesterol in these same structures (Figures 5A and 5B). This was in contrast with neighbouring untransfected cells that showed normal cholesterol staining in much smaller

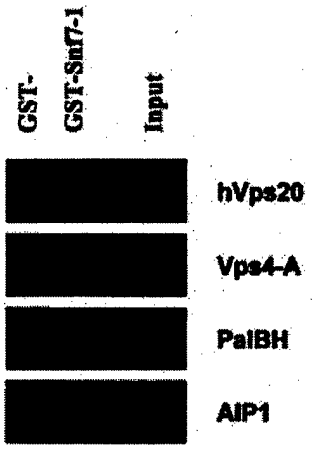

Figure 6 hSnf7-1 binding to candidate proteins as detected by GST-affinity chromatography

Recombinant constructs for epitope-tagged hVps20, Vps4-A, PalBH and AIP1. These proteins were expressed in Cos1 cells, lysates prepared and tested for binding to immobilized GST and GST-hSnf7-1. After washing, the amount of bound protein was analysed by Western blot as described in the Materials and methods section. Part (1/15) of the protein extracts was also electrophoresed on each SDS/polyacrylamide gel to show the input available for binding.

punctuated structures (Figures 5A and 5B). Unexpectedly, a similar, but less dramatic, result was also observed when hVps20 was expressed in cells (Figures 5C and 5D). Specifically, in cells expressing a high level of hVps20, as shown in Figures 5(C) and 5(D), a marked accumulation of large structures staining for cholesterol was observed. Furthermore, cells co-expressing both hSnf7 and Vps20 proteins also showed the accumulation of large vesicular structures containing cholesterol (results not shown). Taken together, these results suggest that hSnf7 proteins and hVps20 function in cholesterol trafficking and probably regulate the trafficking of other cell-surface receptors.

hSnf7 proteins interact with AIP1, but not Vps4-A, PalBH or Vps20

In large-scale yeast two-hybrid screens, Snf7p was found to interact with multiple proteins, including Vps4p [9,10], the calpain protease Rim13p [9] and a Bro1-domain-containing protein, Rim20p [9]. To determine if the mammalian counterparts of these yeast proteins have similar interaction abilities, we used an affinity-capture approach. In addition, we tested whether hVps20 might interact directly with hSnf7 proteins. For these experiments, we produced epitope-tagged proteins in mammalian cells, including hVps20, Vps4-A (a rat homologue of Vps4p [27]) PalBH [22] (a human calpain protease homologue of Rim13p) and AIP1 (a human Bro1-domain-containing homologue of yeast Rim20p [15,16]). Western-blot analysis of Cos1 cells transfected with hVps20, Vps4-A, PALBH and AIP1 mammalian expression vectors revealed that all of these proteins were expressed and migrated at approx. 35, 55, 110 and 90 kDa respectively, as expected for their predicted molecular masses (Figure 6). We tested the ability of recombinant GST-hSnf7-1, immobilized to glutathione beads, to bind these epitope-tagged proteins in Cos1 cell extracts. We found that AIP1 interacted strongly with GST-hSnf7-1, but not with GST (Figure 6). Whereas hVps20, Vps4-A or PalBH were expressed at relatively high levels, they did not significantly interact with immobilized GST-hSnf7-1 (Figure 6). Additional studies showed that both GST-hSnf7-2 and GST-hSnf7-3 also interacted with AIP1 but not Vps4-A (results not shown). The inverse experiments using

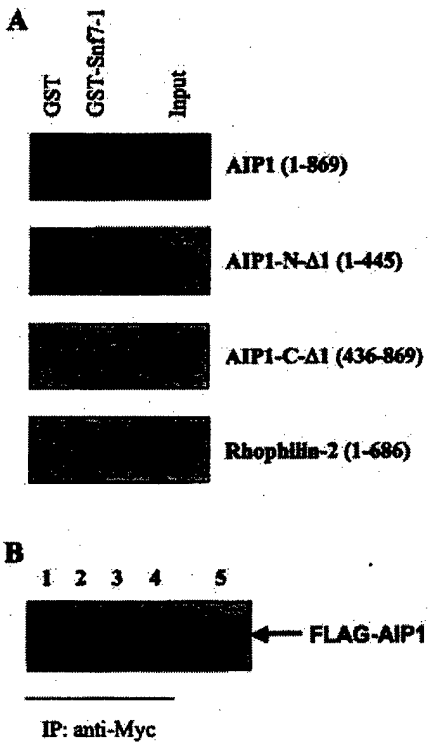

Figure 7 Requirement of the N-terminus of AIP1 for *in vivo* interactions with Snf7-1

(**A**) Immobilized GST or GST-Snf7-1 was incubated with whole cell lysates of Cos-1 cells transfected with FLAG-tagged constructs for AIP1 (amino acids 1–869), AIP1-N-Δ1 (1–445), AIP1-C-Δ1 (436–869) or the human Bro1-containing protein, RPH-2 (1–686). After washing, the amount of FLAG-tagged proteins bound to the immobilized capture proteins was analysed by Western blot as described in the Materials and methods section. Part of the extract (1/50) was also electrophoresed on each SDS/polyacrylamide gel to show the relative inputs for each FLAG-tagged protein. (**B**) Co-immunoprecipitation of AIP1 and Snf7-1 *in vivo*. Cell lysates were prepared from untransfected cells (lane 1), cells transfected with pcDNA-Myc vector and FLAG-tagged AIP1 (lane 2), cells transfected with pcDNA-Myc-tagged hSnf7-1 and FLAG-tagged RPH-2 (lane 3) or cells transfected with pcDNA-Myc-tagged hSnf7-1 and FLAG-tagged AIP1 (lane 4). Immunoprecipitations were performed overnight with a mouse anti-Myc monoclonal antibody as described in the Materials and methods section. The AIP1 input from cells transfected with FLAG-tagged AIP1 is shown as reference (lane 5). After immunoprecipitation, samples were subjected to Western blot and probed with the M2 anti-FLAG™ monoclonal antibody to detect FLAG-tagged AIP1 protein.

GST-Vps4-A and GST-hVps20 left immobilized on glutathione beads also failed to detect interactions with epitope-tagged hSnf7-1 or AIP1 in Cos1 cell extracts (results not shown). Thus our GST affinity-capture approach could detect only one of the known homologous yeast interactions, that of the interaction between hSnf7 proteins and AIP1.

The interaction of hSnf-1 with AIP1 requires the N-terminus of AIP1 and occurs *in vivo*

To map the domain of AIP1 required for interaction with hSnf7-1, we generated two AIP1 deletions, including AIP1-N-Δ1, containing amino acid residues 1–445, and AIP1-C-Δ1, containing amino acid residues 436–869, and tested their ability to bind GST-hSnf7-1. Using Cos1 cell extracts containing these two AIP1-deletion mutant proteins with immobilized GST-hSnf7-1 revealed that the N-terminal half of AIP1 was both necessary and sufficient for interacting with Snf7-1 (Figure 7A), whereas the C-terminal half of AIP1 was unable to bind hSnf7-1 (Figure 7A). Since the N-terminal half of AIP1 contains a Bro1 domain, we tested whether another Bro1-containing protein, RPH-2, could interact with AIP. Whereas RPH-2 was highly expressed, no interaction with AIP1 was detected (Figure 7A). Unfortunately, our attempts to express two additional AIP1 mutants, AIP1-N-Δ2 (amino acids 1–208) and AIP1-N-Δ3 (amino acids 182–445), in mammalian cells or as GST-fusion proteins in *E. coli* failed. As an alternative strategy, we subcloned the three AIP1 N-terminus containing deletion mutants into the pMAL vector system producing maltose-binding protein-fusion proteins. In this system, we were able to express recombinant AIP1-N-Δ1, AIP1-N-Δ2 and AIP1-N-Δ3 (results not shown). Next, we overexpressed Myc-tagged hSnf7-1 in Cos1 cells and performed *in vitro* binding assays with the AIP1 mutants. In these assays, hSnf7-1 bound to AIP1-N-Δ1 (amino acids 1–445), but not to AIP1-N-Δ2 (amino acids 1–208) or AIP1-N-Δ3 (amino acids 182–445) (results not shown). These results suggest that either the AIP1–Snf7-1 interaction requires both the Bro1 and α-helical domain or that the interaction is conformation-dependent and the AIP1-N-Δ2 and AIP1-N-Δ3 mutants have conformations that prohibit hSnf7-1 binding.

Using immunoprecipitation experiments, we also looked for an association between hSnf7-1 and AIP1 in intact cells. Cos1 cells were co-transfected with expression vectors encoding Myc-tagged hSnf7-1 and either FLAG-tagged AIP1 or FLAG-tagged RPH-2. Lysates were prepared 2 days after transfection, and Myc-tagged hSnf7-1 was pulled down using anti-Myc antibody and Protein A/G–agarose beads. The bound proteins were then analysed by Western blotting with anti-FLAG antibody to detect hSnf7-associated proteins (Figure 7B). hSnf7-1 bound full-length AIP1, but not RPH-2 or vector controls (Figure 7B). Since comparable amounts of FLAG-tagged AIP1 and RPH-2 were present in the whole cell lysates (results not shown), these results indicate that the interaction of hSnf7-1 is specific for AIP1.

hSnf7-1 recruits AIP1 to hSnf7-containing late endosomes/lysosomes

We next investigated the relationship between Snf7-1 and AIP1 in HeLa cells by immunofluorescence. When FLAG epitope-tagged AIP1 was expressed in HeLa cells, it exhibited a diffuse cytoplasmic localization, with no detectable vesicular staining (Figures 8A and 8B). When AIP1 and hSnf7-1 were co-transfected in HeLa cells, some of the AIP1 co-localized with Snf7-1 in the late endosomal/lysosomal vesicles (Figures 8C and 8D). Consistent with our binding data, expression of the N-terminus of AIP1 (AIP1-N-Δ1) also co-localized with hSnf7-1 (Figures 8E and 8F). Whereas expression of the C-terminus of AIP1 (AIP1-C-Δ1) either alone or when co-transfected with Snf7-1 did not co-localize with hSnf7-1, it did show a vesicular staining pattern (results not shown). Taken together, these results suggest that AIP1 may reside normally with hSnf7 proteins and function as part of the MVB machinery.

DISCUSSION

The yeast class E Vps proteins such as Snf7p, Vps20p, Vps31/Bro1p and Rim20p form multi-molecular protein complexes that regulate protein trafficking from late endosomes to the lysosome [2]. In the present study, we identified three human homologues of yeast Snf7p and one human homologue of Vps20p. Structurally, human and yeast Snf7 and Vps20 homologues are highly conserved and are predicted to contain a number of α-helical coiled-coil domains that are often involved in protein–protein interactions. The finding of multiple Snf7 proteins in humans

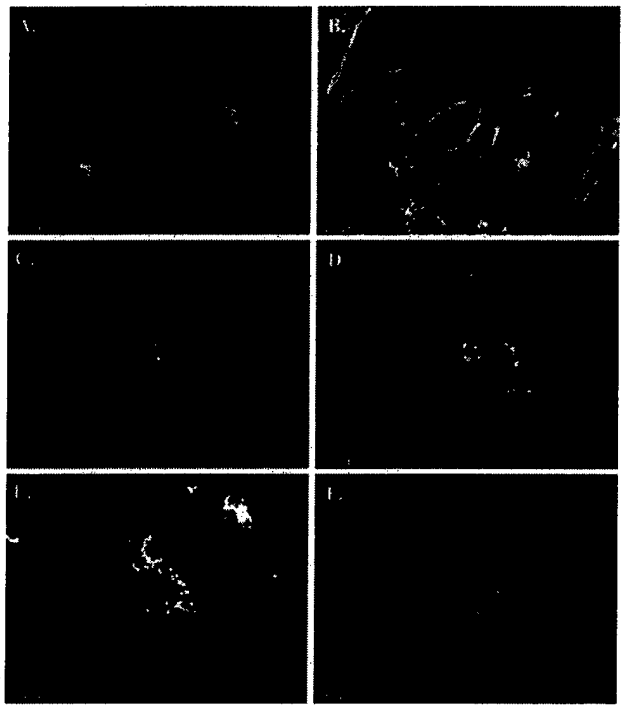

Figure 8 Vesicular co-localization of hSnf7-1 and AIP1

HeLa cells were transfected with FLAG-tagged AIP1 (**A**), co-transfected with Myc epitope-tagged hSnf7-1 (**C**) and FLAG-tagged AIP1 (**D**), Myc epitope-tagged hSnf7-1 (**E**) and FLAG-tagged AIP1-N-Δ1 (**F**). Expressing cells were fixed and treated with anti-epitope antibodies 24 h post-transfection, followed by staining with FITC-conjugated goat anti-rabbit and Texas Red-conjugated goat anti-mouse antibodies. Actin was visualized by staining with Texas Red-conjugated phalloidin (**B**).

versus those in yeast suggests a greater level of complexity in humans. Although we still do not know the exact biological relevance of the different hSnf7 isoforms, they may show cell- or tissue-specific expression and/or function.

Using transfection analysis, we found that overexpressed hSnf7 proteins localized to late endosomes/lysosomes, whereas hVps20 localized to earlier-stage endosomes. Since hSnf7s do not have a consensus myristoylation sequence, myristoylation of hVps20 could provide a biochemical explanation for these localization differences. Interestingly, yeast studies suggest that myristoylated Vps20 and Snf7p are part of a complex *in vivo* and that Vps20p–membrane association is needed for assembling these ESCRT-III structures [6]. We also found that overexpressed hSnf7 proteins and hVps20 markedly impaired cholesterol trafficking, similar to the effect of an ATPase-defective mutant of Vps4-A [26]. In the light of a recent study showing that most of the cholesterol normally resides in multi-vesicular bodies and not in the lysosome [28], a probable explanation is that overexpressed hSnf7 and hVps20 proteins act in a dominant-negative fashion to disrupt the normal protein complexes required for the sorting of cholesterol in these recycling compartments. Our immunofluorescence results are also consistent with the possibility that hSnf7 and hVps20 proteins may be part of large vesicular complexes *in vivo*, although both mammalian and bacterially produced hSnf7 and hVps20 failed to interact directly using *in vitro* binding assays. One explanation might be that these proteins are normally part of the same complex *in vivo*, but require additional components for assembling this complex. Our recombinant-tagged constructs of hVps20 and hSnf7 proteins should be useful for identifying such additional components, which should facilitate a greater understanding of human late endosome/lysosome fusion and the human endocytic transport pathway.

We have already identified a probable physiological binding partner for the hSnf7 proteins. As a starting point in these studies, we utilized data from genome-wide yeast two-hybrid screens showing that Snf7p can interact with Vps4p, Rim13p and Rim20p. By testing mammalian homologues of each of these proteins, we found that only the Snf7–AIP1 interaction, equivalent to the Snf7p–Rim20p interaction, could be detected in our assays using mammalian cell extracts. There are several possible technical and/or biological reasons for not also detecting interactions of hSnf7 with Vps4-A and PalBH. First, some of these yeast interactions may represent false positives, since these interactions were detected using large-scale yeast two-hybrid analysis and were not confirmed independently. Secondly, interactions between Snf7p and Vps4p or Rim13p/PalBH either may not be conserved in mammals or may require additional components. Nevertheless, the finding that hSnf7 proteins interact with AIP1 *in vitro* and *in vivo* is consistent with yeast two-hybrid analysis showing that a putative *A. nidulans* homologue of Snf7p also interacts with human AIP1 [12]. We have also mapped the hSnf7–AIP1 interaction site to the N-terminal half of AIP1. This N-terminal region of AIP1, previously of unknown function, contains both a Brol domain and a coiled-coil region that individually failed to interact with hSnf7. Although the biological and biochemical functions of Brol domains are not known, our results suggest that the Brol domain in AIP1 is probably required for hSnf7 binding. However, another human Brol-containing protein, RPH-2, failed to interact with either of the hSnf7 proteins tested. Our immunofluorescence studies showing a cytoplasmic distribution of AIP1 when overexpressed alone are consistent with previous studies [15,19]. In contrast, we found that co-expression of AIP1 with Snf7 markedly recruited AIP1 to vesicular structures that appear to be late endosomes/lysosomes. These results are in agreement with studies in yeast showing that Snf7 can recruit Brolp, a probable yeast counterpart of AIP1, to endosomes [29]. In addition, our results may help explain recent proteonomic data indicating that endogenous AIP1 may normally reside in vesicular structures such as phagosomes [30] and in exosomes derived from MVBs [31]. Although Snf7 proteins were not detected in these proteonomic studies, it is probable that Snf7 proteins play important roles in regulating the levels of AIP1 in those structures. In the light of the ability of the C-terminus of AIP1 to bind endophilin and induce vacuolization [19], our observation that overexpressed Snf7s accumulate in and promote the formation of large cholesterol-containing vesicles suggests that AIP1 may play a central role in MVB function. Finally, based on known interactions between ESCRT-III components in yeast [5], we predict that future studies in mammalians cells will show that hVps20–hSnf7 complexes interact directly or indirectly with human homologues of Vps2 and Vps24.

Recently, Katoh et al. [25] identified two AIP1/ALIX-interacting proteins via yeast two-hybrid screening, termed CHMP4s, which are identical with the Snf7s described in the present study. These authors also observed that the Brol domain of AIP1/ALIX was required but not sufficient for interaction with human CHMP4/Snf7 proteins. However, unlike the observations of Katoh et al. [25], we did not observe CHMP4/Snf7 proteins to co-localize with EEA1-positive early endosomes, but rather to localize to late-stage endosomes/lysosomes. The reason for this discrepancy in localization is unknown, but could be due to differences in culture conditions or levels of transfected proteins. Nevertheless, the finding that overexpressed Snf7/CHMP4 proteins alter EGF trafficking [25] and cholesterol trafficking is consistent with

yeast studies showing a role for these proteins in protein sorting [4,5]. Together, these studies support a critical, evolutionarily conserved role of Snf7, Vps20 and AIP1/Bro1p proteins in protein trafficking.

This work was supported by a grant from NCI-R29 CA422142 to P. D. B. and a DOD breast cancer predoctoral fellowship to J. W. P. We also thank the Microscopy and Imaging Shared Resources of Lombardi Cancer Center, which is partially supported by National Institute of Health Grant 1P30-CA-51008 (Cancer Center Support Grant, to Lombardi Cancer Center).

REFERENCES

1 Mellman, I. (1996) Endocytosis and molecular sorting. Annu. Rev. Cell Dev. Biol. **12**, 575–625
2 Katzmann, D. J., Odorizzi, G. and Emr, S. D. (2002) Receptor downregulation and multivesicular-body sorting. Nat. Rev. Mol. Cell Biol. **3**, 893–905
3 Raymond, C. K., Howald-Stevenson, I., Vater, C. A. and Stevens, T. H. (1992) Morphological classification of the yeast vacuolar protein sorting mutants: evidence for a prevacuolar compartment in class E vps mutants. Mol. Biol. Cell **3**, 1389–1402
4 Babst, M., Katzmann, D. J., Snyder, W. B., Wendland, B. and Emr, S. D. (2002) Endosome-associated complex, ESCRT-II, recruits transport machinery for protein sorting at the multivesicular body. Dev. Cell **3**, 283–289
5 Babst, M., Katzmann, D. J., Estepa-Sabal, E. J., Meerloo, T. and Emr, S. D. (2002) Escrt-III: an endosome-associated heterooligomeric protein complex required for mvb sorting. Dev. Cell **3**, 271–282
6 Kranz, A., Kinner, A. and Kolling, R. (2001) A family of small coiled-coil-forming proteins functioning at the late endosome in yeast. Mol. Biol. Cell **12**, 711–723
7 Tu, J., Vallier, L. G. and Carlson, M. (1993) Molecular and genetic analysis of the SNF7 gene in *Saccharomyces cerevisiae*. Genetics **135**, 17–23
8 Gavin, A. C., Bosche, M., Krause, R., Grandi, P., Marzioch, M., Bauer, A., Schultz, J., Rick, J. M., Michon, A. M., Cruciat, C. M. et al. (2002) Functional organization of the yeast proteome by systematic analysis of protein complexes. Nature (London) **415**, 141–147
9 Ito, T., Chiba, T., Ozawa, R., Yoshida, M., Hattori, M. and Sakaki, Y. (2001) A comprehensive two-hybrid analysis to explore the yeast protein interactome. Proc. Natl. Acad. Sci. U.S.A. **98**, 4569–4574
10 Uetz, P., Giot, L., Cagney, G., Mansfield, T. A., Judson, R. S., Knight, J. R., Lockshon, D., Narayan, V., Srinivasan, M., Pochart, P. et al. (2000) A comprehensive analysis of protein–protein interactions in *Saccharomyces cerevisiae*. Nature (London) **403**, 623–627
11 Xu, W. and Mitchell, A. P. (2001) Yeast PalA/AIP1/Alix homolog Rim20p associates with a PEST-like region and is required for its proteolytic cleavage. J. Bacteriol. **183**, 6917–6923
12 Vincent, O., Rainbow, L., Tilburn, J., Arst, Jr, H. N. and Penalva, M. A. (2003) YPXL/I is a protein interaction motif recognized by *Aspergillus* PalA and its human homologue, AIP1/Alix. Mol. Cell. Biol. **23**, 1647–1655
13 Negrete-Urtasun, S., Denison, S. H. and Arst, Jr, H. N. (1997) Characterization of the pH signal transduction pathway gene PalA of *Aspergillus nidulans* and identification of possible homologs. J. Bacteriol. **179**, 1832–1835
14 Che, S., El-Hodiri, H. M., Wu, C. F., Nelman-Gonzalez, M., Weil, M. M., Etkin, L. D., Clark, R. B. and Kuang, J. (1999) Identification and cloning of xp95, a putative signal transduction protein in *Xenopus* oocytes. J. Biol. Chem. **274**, 5522–5531
15 Vito, P., Pellegrini, L., Guiet, C. and D'Adamio, L. (1999) Cloning of AIP1, a novel protein that associates with the apoptosis-linked gene ALG-2 in a Ca^{2+}-dependent reaction. J. Biol. Chem. **274**, 1533–1540
16 Missotten, M., Nichols, A., Rieger, K. and Sadoul, R. (1999) Alix, a novel mouse protein undergoing calcium-dependent interaction with the apoptosis-linked-gene 2 (ALG-2) protein. Cell Death Differ. **6**, 124–129
17 Wu, Y., Pan, S., Che, S., He, G., Nelman-Gonzalez, M., Weil, M. M. and Kuang, J. (2001) Overexpression of Hp95 induces G1 phase arrest in confluent HeLa cells. Differentiation **67**, 139–153
18 Chen, B., Borinstein, S. C., Gillis, J., Sykes, V. W. and Bogler, O. (2000) The glioma-associated protein SETA interacts with AIP1/Alix and ALG-2 and modulates apoptosis in astrocytes. J. Biol. Chem. **275**, 19275–19281
19 Chatellard-Causse, C., Blot, B., Cristina, N., Torch, S., Missotten, M. and Sadoul, R. (2002) Alix (ALG-2-interacting protein X), a protein involved in apoptosis, binds to endophilins and induces cytoplasmic vacuolization. J. Biol. Chem. **277**, 29108–29115
20 Borinstein, S. C., Hyatt, M. A., Sykes, V. W., Straub, R. E., Lipkowitz, S., Boulter, J. and Bogler, O. (2000) SETA is a multifunctional adapter protein with three SH3 domains that binds Grb2, Cbl, and the novel SB1 proteins. Cell Signal. **12**, 769–779
21 Peck, J. W., Oberst, M., Bouker, K. B., Bowden, E. and Burbelo, P. D. (2002) The RhoA-binding protein, rhophilin-2, regulates actin cytoskeleton organization. J. Biol. Chem. **277**, 43924–43932
22 Futai, E., Kubo, T., Sorimachi, H., Suzuki, K. and Maeda, T. (2001) Molecular cloning of PalBH, a mammalian homologue of the *Aspergillus* atypical calpain PalB. Biochim. Biophys. Acta **1517**, 316–319
23 Burbelo, P. D., Drechsel, D. and Hall, A. (1995) A conserved binding motif defines numerous candidate target proteins for both Cdc42 and Rac GTPases. J. Biol. Chem. **270**, 29071–29074
24 Howard, T. L., Stauffer, D. R., Degnin, C. R. and Hollenberg, S. M. (2001) CHMP1 functions as a member of a newly defined family of vesicle trafficking proteins. J. Cell Sci. **114**, 2395–2404
25 Katoh, K., Shibata, H., Suzuki, H., Nara, A., Ishidoh, K., Kominami, E., Yoshimori, T. and Maki, M. (2003) The ALG-2-interacting protein Alix associates with CHMP4b, a human homologue of yeast Snf7 that is involved in multivesicular body sorting. J. Biol. Chem. **278**, 39104–39113
26 Bishop, N. and Woodman, P. (2000) ATPase-defective mammalian VPS4 localizes to aberrant endosomes and impairs cholesterol trafficking. Mol. Biol. Cell **11**, 227–239
27 Babst, M., Wendland, B., Estepa-Sabal, E. J. and Emr, S. D. (1998) The Vps4p AAA ATPase regulates membrane association of a Vps protein complex required for normal endosome function. EMBO J. **17**, 2982–2993
28 Mobius, W., van Donselaar, E., Ohno-Iwashita, Y., Shimada, Y., Heijnen, H. F., Slot, J. W. and Geuze, H. J. (2003) Recycling compartments and the internal vesicles of multivesicular bodies harbor most of the cholesterol found in the endocytic pathway. Traffic **4**, 222–231
29 Odorizzi, G., Katzmann, D. J., Babst, M., Audhya, A. and Emr, S. D. (2003) Bro1 is an endosome-associated protein that functions in the MVB pathway in *Saccharomyces cerevisiae*. J. Cell Sci. **116**, 1893–1903
30 Garin, J., Diez, R., Kieffer, S., Dermine, J. F., Duclos, S., Gagnon, E., Sadoul, R., Rondeau, C. and Desjardins, M. (2001) The phagosome proteome: insight into phagosome functions. J. Cell Biol. **152**, 165–180
31 Thery, C., Boussac, M., Veron, P., Ricciardi-Castagnoli, P., Raposo, G., Garin, J. and Amigorena, S. (2001) Proteomic analysis of dendritic cell-derived exosomes: a secreted subcellular compartment distinct from apoptotic vesicles. J. Immunol. **166**, 7309–7318

Received 3 September 2003/13 October 2003; accepted 29 October 2003
Published as BJ Immediate Publication 29 October 2003, DOI 10.1042/BJ20031347